Unsupervised linear unmixing of hyperspectral image for crop yield estimation

Bin Luo
GIPSA-Lab, Grenoble Institute of Technology
Grenoble, France
Bin.luo@gipsa-lab.inpg.fr

Chenghai Yang
USDA-ARS
Weslaco, TX, USA
chenghai.yang@ars.usda.gov

Jocelyn Chanussot
GIPSA-Lab, Grenoble Institute of Technology
Grenoble, France
Jocelyn.Chanussot@gipsa-lab.inpg.fr

***Abstract*—Multispectral and hyperspectral imagery are often used for estimating crop yield. This paper describes an unsupervised unmixing scheme of hyperspectral images on field in order to estimate the crop yield. From the hyperspectral images, the endmembers and their abundance maps are computed by unsupervised unmixing. The abundance maps are then compared with the crop yield data. The results show the capability for estimating crop yield of the unmixing scheme, thanks to the high correlations between the crop yield data and the abundance maps of the endmembers corresponding to crop, even though the scheme is totally unsupervised.**

I. Introduction

Multispectral and hyperspectral imagery are often used for estimating crop yield. Traditionally, the crop field yield is estimated by some vegetation index from the images [1][2]. These index are often computed from certain combinations of visible and near-infrared bands, of which the most famous may be NDVI=(NIR-Red)/(NIR+Red) [3]. The high correlation between the vegetation index and the ground truth crop yield data shows the capability of the vegetation index for estimating crop yield.

Hyperspectral imagery, which often contains hundreds of spectral bands, has been evaluated for crop yield estimation in [4][5]. These almost continuous spectra, which provide much more spectral information on the observed materials, have the potential to better describe the biological and chemical attributes of the plants. The spatial abundance of the vegetation on a scene derived from hyperspectral image can be more precise than the vegetation index deduced from multispectral image. Recently, it was proposed to compute the vegetation abundance in order to map the crop yield with the help of linear unmix of hyperspectral images in [6]. The authors assume that the spectrum of a pixel in the hyperspectral image on a crop field is a linear mixture of the spectra of vegetation and bare soil. The abundance of vegetation is then calculated by using linear regression. In [6], the spectra of vegetation and bare soil are supposed to be known. They are either measured in laboratory or selected manually from the image. This is a main drawback of the method, since the reference spectrum is not always available. Moreover, the hypothesis which supposes the spectrum of a pixel is a linear mixture of only two endmembers (vegetation and bare soil) is questionable, since other endmembers can be present (for example asphalt, if there are roads between the fields).

Therefore, in this paper, we present a totally blind linear unmixing scheme for hyperspectral images which is applied for crop field yield estimation. For all the linear unmixing methods, one has always to manually fix the number of endmembers at first. Therefore, the first step of the unmixing scheme consists in estimating the sub space dimension of the endmembers which span the hyperspectral image. In [7], a method to estimate the number of endmembers based on the distribution of eigenvalues of the correlation and covariance matrix of the data has been proposed. The experiments in [7] show that this method works very precisely, even though the hyperspectral images may be affected by the artifacts. For linear unmixing of hyperspectral images, one can find two families of approaches: statistical methods (such as the Independent Component Analysis [8], Bayesian Positive Source Separation [9], etc.) and geometrical methods (such as N-Finder [10], VCA [11], etc.). In this paper, we use the geometrical method - Vertex Component Analysis (VCA) to unmix the hyperspectral image. With the help of the unsupervised unmixing scheme, we can obtain the abundance map of vegetation without any manual processing and any information *a piori* on the crop. The correlation coefficient computed between the abundance of vegetation and the ground truth crop yield data will show the capability of the scheme for estimating crop yield.

The outline of this paper is as follow: in Section II, we present the linear mixture model of hyperspectral image. In Section III-A and III-B, we present very briefly the approach used for estimating the number of endmembers and the linear unmixing approach (VCA) respectively. In Section IV, we present the mapping results obtained on a real hyperspectral data set. Finally, we conclude in Section V.

II. Linear mixture model

We note $\mathbf{X}$ the matrix representing the hyperspectral image cube, where $\mathbf{X} = \{\mathbf{x}_1, \mathbf{x}_2, \ldots, \mathbf{x}_{N_a}\}$ and $\mathbf{x}_k = \{x_{1,k}, x_{2,k}, \ldots, x_{N_s,k}\}^T$, $x_{l,k}$ is the value of the kth pixel at the lth band. We assume that the spectrum of each pixel is a linear mixture of the spectra of N_c endmembers, leading to the following model:

$$\mathbf{X} = \mathbf{MS} + \mathbf{n} \tag{1}$$

where $\mathbf{M} = \{\mathbf{m}_1, \mathbf{m}_2, \ldots, \mathbf{m}_{N_c}\}$ is the mixing matrix where $\mathbf{m}_n$ denotes the spectral signature of the nth endmember. $\mathbf{S} = \{\mathbf{s}_1, \mathbf{s}_2, \ldots, \mathbf{s}_{N_c}\}^T$ is the abundance matrix where $\mathbf{s}_n = \{s_{n,1}, s_{n,2}, \ldots, s_{n,N_a}\}$ ($s_{n,k} \in [0,1]$ is the abundance of the nth endmember at the kth pixel). $\mathbf{n}$ stands for the additive noise of the image. For separating $\mathbf{M}$ and $\mathbf{S}$ from $\mathbf{X}$ without any *a priori* information, we first have to estimate the number N_c of endmembers . In a second step, we can perform a linear unmixing in order to obtain $\mathbf{M}$ and $\mathbf{S}$.

III. Linear unmixing of hyperspecytral images

A. Estimation of the number of endmembers

in [7], the authors have proposed an approach for estimating the number of endmembers by using the eigenvalues of the correlation and covariance matrix of the hyperspectral image. In this section, we briefly introduce the main idea of this method. We note K the sample covariance matrix of $\mathbf{X}$ and R its correlation matrix. Suppose that λ_i and $\hat{\lambda}_i$ are respectively the ith eigenvalues of K and R with $i \geq 0$, $\lambda_i > \lambda_{i+1}$ and $\hat{\lambda}_i > \hat{\lambda}_{i+1}$. Theoretically, if there are N_c endmembers present in $\mathbf{X}$, the eigenvalues $\hat{\lambda}_i, (i > N_c)$ and $\lambda_i, (i > N_c)$ correspond to the noise variance. Noting $z_i = \hat{\lambda}_i - \lambda_i$, the distribution of z_i can be asymptotically modeled by [12][13]:

$$\begin{array}{ll} z_i \sim \aleph(\mu_i, \sigma_i^2), & i \leq N_c \\ z_i \sim \aleph(0, \sigma_i^2), & i > N_c \end{array} \tag{2}$$

where μ_i is unknown and σ_i can be given by $\sigma_i^2 \approx \frac{2}{N}(\hat{\lambda}_i^2 + \lambda_i^2)$, if the number of samples is sufficiently large (which is usually the case for hyperspectral images).

Based on Equation 2, the authors of [7] proposed to calculate the likelihhood function of z_i of which the position of the *maximum* corresponds to the number of endmembers N_c. Moreover, the authors of [7] found that if there are some bands which are corrupted by artifacts, the number of endmembers N_c corresponds the position of the first local *maximum*.

B. Vertex Component Analysis (VCA)

In [11], the Vertex Component Analysis (VCA) is proposed as an effecient method for extracting the endmembers which are linearly mixed. The main idea is to extract the vertex of the simplex formed by $\mathbf{M}$ which contains all the data vectors in $\mathbf{X}$. According to the sum-to-one condition, the sum of the abundances of all the endmembers for each pixel is equal to one, *i.e.* $\forall k, \sum_{n=1}^{N_c} s_{n,k} = 1$. Therefore the data vectors $\mathbf{x}_l$ are always inside a simplex of which the vertex are the spectra of the endmembers if there is no noise. VCA iteratively projects the data onto the direction orthogonal to the subspace spanned by the endmembers already determined. And the extremity of this projection is the new endmember signature. The algorithm stops when p endmembers are extracted, where p is the number of endmembers which has to be fixed before performing VCA. In practice, we fix p by the number of endmembers determined by the approach presented in Section III-A. We note $\hat{\mathbf{M}} = \{\hat{\mathbf{m}}_1, \ldots, \hat{\mathbf{m}}_p\}$ the spectra of the endmembers extracted by VCA. The abundance maps $\hat{\mathbf{S}} = \{\hat{\mathbf{s}}_1, \ldots, \hat{\mathbf{s}}_p\}$ of the endmembers are then obtained by

$$\hat{\mathbf{S}} = \mathbf{X} \times \hat{\mathbf{M}}^{-1}. \tag{3}$$

Remark that since the only parameter to be fixed, the number of endmembers, can be determined by the method introduced in III-A, which is also unsupervised, the linear unmixing scheme is totally parameter free. By using this scheme, without any information *a priori* on the endmembers, we can extract the spectra and the abundance maps of the endmembers in a hyperspectral image.

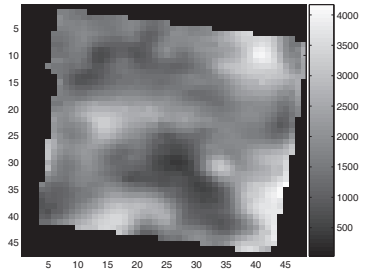

Fig. 1. Crop yield data with 8.7m spatial resolution.

IV. Experiments and results

In this section, the scheme of linear unmixing presented in Section III is applied for extracting the spectra and abundance maps of the endmembers in a hyperspectral image taken on a crop field. The correlation coefficients are then computed between the abundance maps and the crop yield data. For comparing our approach with the state of the art method proposed in [6], we use the same hyperspectral image (Field one in Figure 3 of [6]). It was acquired from the fields with an airborne hyperspectral imaging system mounted on a Cessna 206 single-engine aircraft. The system was configured to record 12-bit imagery with 128 bands over the spectral range from 457.2 nm to 921.7 nm at 3.63 nm intervals. The image was recorded under sunny and calm conditions from the field after the crop had reached the soft to hard dough stages and achieved its maximum canopy cover. The swath of the image was approximately 840 m and the ground pixel size was 1.3 m. Because of the low quantum efficiency near the NIR end of the observed spectrum, only 102 bands with wavelengths from 477.2 nm to 843.7 nm were used.

Yield data (Figure 1), serving as ground truth, were recorded with an Ag Leader PF3000 yield monitor (Ag Leader Technology, Ames, Iowa), which was calibrated to ensure accuracy before the grain was harvested. The used combine had an effective cutting width of 8.7 m, which is therefore the spatial resolution of the yield data.

The approach introduced in Section III-A is used for estimating the number of endmembers, which is $p = 5$. We then use VCA [11] (see Section III-B) to extract the spectra of the

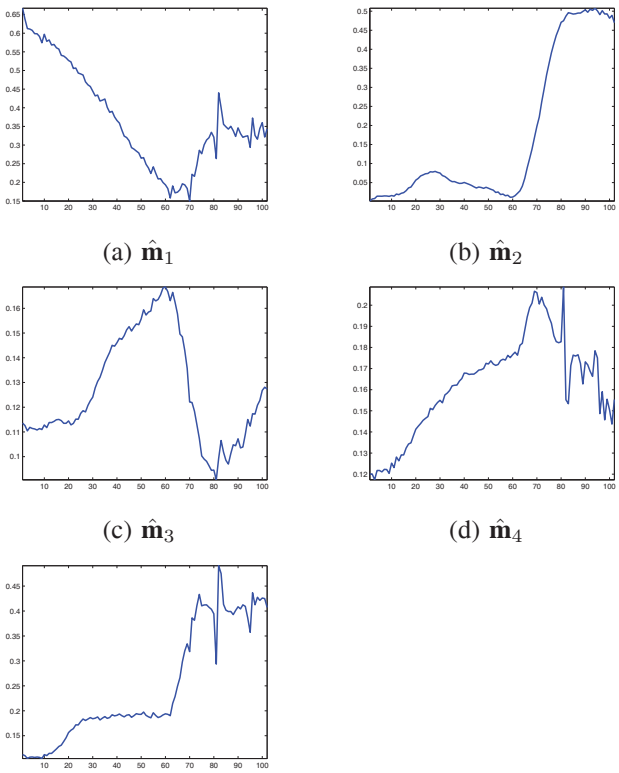

(a) $\hat{\mathbf{m}}_1$ (b) $\hat{\mathbf{m}}_2$ (c) $\hat{\mathbf{m}}_3$ (d) $\hat{\mathbf{m}}_4$ (e) $\hat{\mathbf{m}}_5$

Fig. 2. Spectra of the 5 endmembers extracted by VCA. Remark that the spatial resolution of the abundance maps is the same as the hyperspectral image (1.3m).

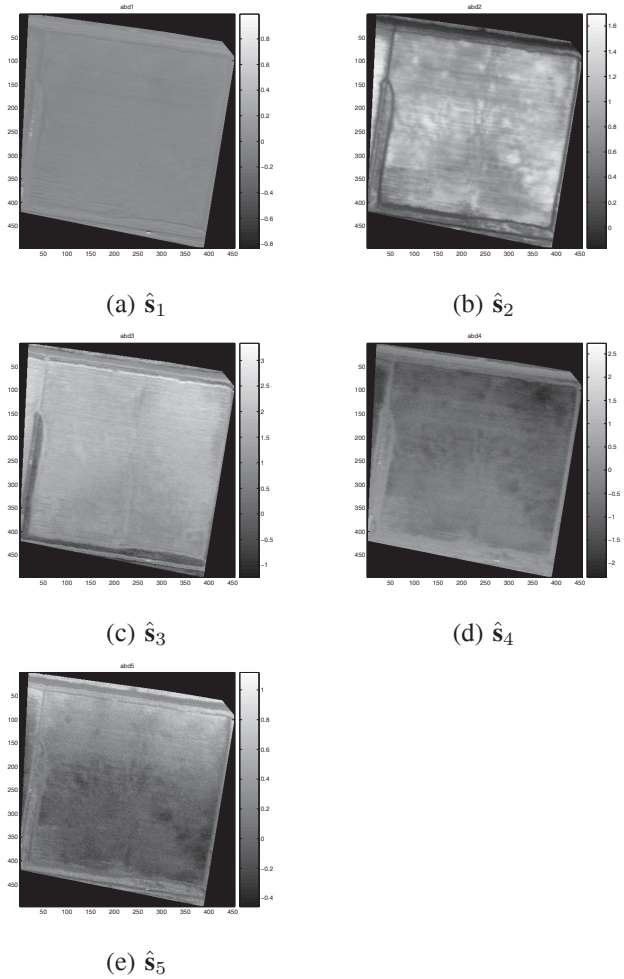

(a) $\hat{\mathbf{s}}_1$ (b) $\hat{\mathbf{s}}_2$ (c) $\hat{\mathbf{s}}_3$ (d) $\hat{\mathbf{s}}_4$ (e) $\hat{\mathbf{s}}_5$

Fig. 3. Abundance maps of the 5 endmembers extracted by VCA.

Abundance	$\hat{\mathbf{s}}_1$	$\hat{\mathbf{s}}_2$	$\hat{\mathbf{s}}_3$	$\hat{\mathbf{s}}_4$	$\hat{\mathbf{s}}_5$
r	0.2570	**0.7239**	0.1960	-0.4014	-0.0558

TABLE I
CORRELATION COEFFICIENT BETWEEN THE ABUNDANCE MAPS AND THE CROP YIELD DATA.

5 endmembers as well as their abundance maps. In Figure 2, the spectra of these endmemebers ($\hat{\mathbf{M}} = \{\hat{\mathbf{m}}_1, \ldots, \hat{\mathbf{m}}_5\}$) are shown. It can be seen that the second endmember (Figure 2(b)) is the most similar to the spectrum of vegetation.

In Figure 3, we have shown the abundance maps of the endmembers ($\hat{\mathbf{S}} = \{\hat{\mathbf{s}}_1, \ldots, \hat{\mathbf{s}}_5\}$) extracted by VCA.

Considering the spatial resolutions of the crop yield data (8.7m) and the abundance maps (1.3m), we have downsampled the abundance maps by the factor $\frac{8.7}{1.3}$ with the help of a bilinear interpolation. For each downsampled abundance map, we have calculated the correlation coefficient r_i between it and the crop yield data (see Table I). It can be observed that the highest correlation coefficient is obtained on the abundance map of the second endmember (see Figure 3(b)), which is the most similar to the vegetation based on the observation of the spectrum shown in Figure 2(b). The high correlation between the crop yield data and the abundance of vegetation shows the capability of the unmixing scheme presented in this paper for estimating the crop yield.

For comparing our approach with the state of the art method in [6], we recall that the authors of [6] computed the correlation between the crop yield data and the vegetation abundance obtained by linear unmixing, assuming that there are only two endmembers: vegetation and bare soil. As discussed in Section I, other endmembers can be present and the approach proposed in [6] requires the reference spectra of vegetation and bare soil. These spectra are obtained either by laboratory measurement or by manual extraction from the image. In order to retrieve the reference spectra, many information have to be known beforehand, such as the type of crop, the moisture, etc. The correlation coefficients obtained in [6] on the same data set are respectively equal to 0.63 and 0.62 when the reference spectra of vegetation are obtained by laboratory measurement and manual extraction from the image.

Remark that the result obtained by using the scheme proposed in the paper is better than in [6]. While the proposed scheme is totally unsupervised: it does not require any information *a priori*.

Since there is noise in the hyperspectral data, the abundance values obtained by Equation (3) are not necessarily in the inter-

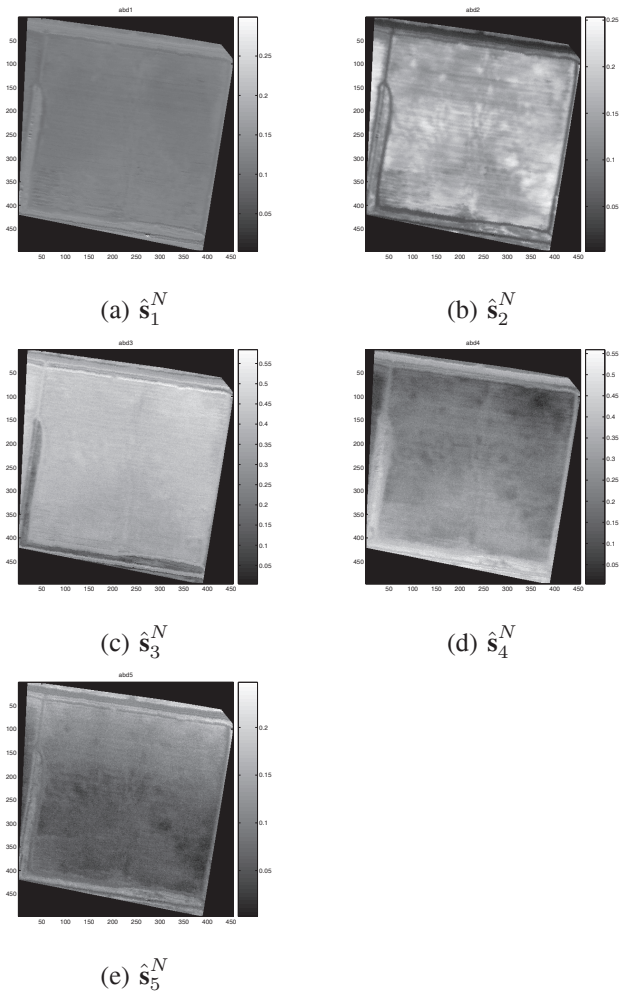

(a) $\hat{\mathbf{s}}_1^N$ (b) $\hat{\mathbf{s}}_2^N$

(c) $\hat{\mathbf{s}}_3^N$ (d) $\hat{\mathbf{s}}_4^N$

(e) $\hat{\mathbf{s}}_5^N$

Fig. 4. Normalised abundance maps of the 5 endmembers extracted by VCA.

Abundance	$\hat{\mathbf{s}}_1^N$	$\hat{\mathbf{s}}_2^N$	$\hat{\mathbf{s}}_3^N$	$\hat{\mathbf{s}}_4^N$	$\hat{\mathbf{s}}_5^N$
r	0.0510	**0.7338**	0.2221	-0.3627	-0.0837

TABLE II
CORRELATION COEFFICIENT BETWEEN THE NORMALISED ABUNDANCE MAPS AND THE CROP YIELD DATA.

val of $[0, 1]$. The normalised abundance maps $\hat{\mathbf{s}}_i^N$ $(i = 1, \ldots, 5)$ are then computed by (see Figure 4):

$$\hat{\mathbf{s}}_i^N = \frac{\hat{\mathbf{s}}_i - \inf \hat{\mathbf{s}}_i}{\sum_{i=1}^{5} (\hat{\mathbf{s}}_i - \inf \hat{\mathbf{s}}_i)}.$$

These normalised abundance maps are then downsampled in order to compute the correlation coefficients between them and the crop yield data, which are shown in Table II.

It can be observed that the normalisation can slightly improve the correlation between the abundance of the vegetation (from 0.7239 to 0.7338) and the crop yield data.

V. Conclusion

In this paper, we have presented a scheme for estimating the crop yield with the help of linear unmixing of hyperspectral images. As the most essential parameter for linear unmixing, the number of endmembers is firstly determined by an approach based on the eigenvalues of the correlation and covariance matrix of hyperspectral data. Afterwards, the spectra and the abundance maps of the endmembers are then extracted by VCA. In order to validate our approach, the experiment is carried out on an airbone hyperspectral image of a real field with crop yield data serving as ground truth. The high correlation between the crop yield data and the abundance of vegetation extracted by the proposed scheme shows its capability for estimating crop yield.

Acknowledgment

This work is funded by French ANR project VAHINE.

References

[1] R. E. Plant, D. Munk, B. Roberts, R. Vargas, D. Rains, R. Travis, and R. Hutmacher, "Relationships between remotely sensed reflectance data and cotton growth and yield," *Transactions of the ASAE*, vol. 43, no. 3, pp. 535–564, 2000.

[2] C. Yang, J. H. Everitt, and J. M. Bradfort, "Relationships between yield monitor data and airborne multispectral," *Precision Agriculture*, vol. 3, no. 4, 2002.

[3] J. Rouse, R. Haas, J. Shell, and D. Deering, "Monitoring vegetation systems in the great plains with erts-1," in *Third Earth Resources Technology Satellite Symposium*, vol. 1, Goddard Washington D.C. USA: Space Flight Cente, 1973, pp. 309–317.

[4] P. Goel, S. Prasher, J. Landry, R. M. Patel, A. Viau, and J. Miller, "Estimation of crop biophysical parameters through airborne and field hyperspectral remote sensing," *Transactions of the ASAE*, vol. 46, no. 4, pp. 1235–1246, 2003.

[5] P. Zarco-Tejada, S. Ustin, and M. Whiting, "Temporal and spatial relationships between within-field yield variability in cotton and high-spatial hyperspectral remote sensing imagery," *Agronomy Journal*, vol. 97, pp. 641–653, 2005.

[6] C. Yang, J. H. Everitt, and J. M. Bradfort, "Airborne hyperspectral imagery and linear spectral," *Precision Agriculture*, vol. 8, no. 7, pp. 279–296, 2007.

[7] B. Luo and J. Chanussot, "Unsupervised hyperspectral image classification by using linear unmixing," in *IEEE ICIP*, Cairo Egypt, 2009.

[8] J. Nascimento and J. B. Dias, "Does independent component analysis play a role in unmixing hyperspectral data," *IEEE Trans. on Geoscience and Remote Sensing*, vol. 43, no. 1, pp. 175–187, 2005.

[9] S. Moussaoui, H. Hauksdóttir, F. Schmidt, C. Jutten, J. Chanussot, D. Brie, S. Douté, and J. Benediktsson, "On the decomposition of mars hyperspectral data by ICA and bayesian positive source separation," *Neurocomputing*, vol. 71, pp. 2194–2208, 2008.

[10] M. E. Winter, "Fast autonomous spectral end-member determination," in *Proc. 13th Int. Conf. on Applied Geologic*, vol. 2, Vancouver Canada, 1999, pp. 337–344.

[11] J. Nascimento and J. B. Dias, "Vertex component analysis: A fast algorithm to unmix hyperspectral data," *IEEE Trans.on Geoscience and Remote Sensing*, vol. 43, no. 4, pp. 898–910, April 2005.

[12] C.-I. Chang and Q. Du, "Estimation of number of spectrally distinct signal," *IEEE Trans. on Geoscience and Remote Sensing*, vol. 42, no. 3, pp. 608–619, 2004.

[13] T. Anderson, *An introduction to multivariate statistical analysis*, 2nd ed. Springer-Verlag, 1984.